

Increasing Ca²⁺ transients by broadening postsynaptic action potentials enhances timing-dependent synaptic depression

Yu-Dong Zhou, Corey D. Acker, Theoden I. Netoff, Kamal Sen, and John A. White*

Department of Biomedical Engineering, Center for Biodynamics, Center for Memory and Brain, Boston University, Boston, MA 02215

Communicated by Nancy J. Kopell, Boston University, Boston, MA, November 12, 2005 (received for review August 12, 2005)

Repeated induction of pre- and postsynaptic action potentials (APs) at a fixed time difference leads to long-term potentiation (LTP) or long-term depression (LTD) of the synapse, depending on the temporal order of pre- and postsynaptic activity. This phenomenon of spike-timing-dependent plasticity (STDP) is believed to arise by nonlinear processes that lead to larger calcium transients (and thus LTP) when presynaptic APs precede postsynaptic APs and smaller calcium transients (and thus LTD) when postsynaptic APs precede presynaptic APs. In contrast to predictions from such calcium-peak-detector models, we show that constitutively or artificially broadened APs in layer II/III pyramidal cells of entorhinal cortex (EC) lead to an increase in the dendritic calcium transient and shift the balance of STDP toward LTD. STDP in entorhinal pyramidal cells is NMDA-receptor-dependent and modulated by the Ca_v1 Ca²⁺ channel-blocker nifedipine. Results are consistent with an elaboration of the calcium-peak-detector model in which downstream signals from voltage-dependent Ca²⁺ channels suppress LTP relative to LTD. Our results suggest that modulation of AP width is a potent way to adjust the rules of synaptic plasticity in the EC.

spike-timing-dependent plasticity | NMDA receptors | nifedipine | calcium imaging | entorhinal cortex

The temporal order of repeated pairing of pre- and postsynaptic action potentials (APs) plays a key role in determining the direction of synaptic plasticity (1–11). This phenomenon of spike-timing-dependent plasticity (STDP) has been shown to be Ca²⁺-dependent (1, 3, 9). Although the details of the underlying Ca²⁺ mechanisms of STDP are not fully understood, it is believed to arise via a calcium-peak-detector model (3, 9, 12–14). In this model, long-term depression (LTD) is induced when presynaptic APs lag postsynaptic APs, generating small dendritic Ca²⁺ transients; and long-term potentiation (LTP) is induced when presynaptic APs precede postsynaptic APs, generating larger Ca²⁺ transients (15).

A key prediction of the peak-detector model is that broader dendritic APs should enhance timing-dependent LTP by increasing the Ca²⁺ flux through NMDA receptors and postsynaptic voltage-gated Ca²⁺ channels. We tested this prediction in layer II/III pyramidal cells of the rat entorhinal cortex (EC), where classical LTP and LTD have been observed in response to periodic stimulation of input fibers (16). We confirmed that EC cells exhibit STDP and found that constitutively or artificially broadened postsynaptic APs lead to an increase in the dendritic calcium transient but shift the balance of STDP toward LTD, in contrast to what one would predict from the peak-detector model. STDP is NMDA receptor-dependent and modulated by the Ca_v1 Ca²⁺ channel-blocker nifedipine. Our results are consistent with an elaboration of the calcium peak-detector model in which downstream signals from voltage-dependent Ca²⁺ channels suppress LTP, making LTD more prominent.

Materials and Methods

Slice Preparation. All protocols were approved by the Boston University Animal Care and Use Committee. Brain slices of EC

were prepared from Long-Evans rats (14–19 days old) as described in ref. 17. Rats were anesthetized with isoflurane, and the brain was removed after decapitation. The EC and hippocampus were dissected rapidly and transferred to a chamber filled with ice-cold oxygenated (95% O₂/5% CO₂) artificial cerebrospinal fluid (126 mM NaCl, 2.5 mM KCl, 1.25 mM NaH₂PO₄, 2 mM MgCl₂, 26 mM NaHCO₃, 25 mM dextrose, and 2 mM CaCl₂). Transverse slices of EC (300 μm) were cut with a tissue slicer (Vibratome 1000 Plus, Ted Pella, Inc., Redding, CA) and incubated at room temperature for at least 1 h before being transferred to the recording chamber at 34–36°C.

Electrophysiological Recording. Whole-cell recordings of layer II/III pyramidal neurons were performed on brain slices of EC. Layer II/III pyramidal neurons were identified under infrared differential interference contrast optics based on their morphology and patched with 4- to 6-MΩ glass pipettes filled with artificial intracellular fluid (120 mM potassium gluconate, 10 mM KCl, 10 mM Hepes, 4 mM Mg-ATP, 0.3 mM Tris-GTP, 10 mM sodium phosphocreatine, and 20 units/ml creatine kinase). Pipettes were connected to the headstage of an AxoClamp 2B amplifier (Axon Instruments, Foster City, CA), and the bridge mode was used to obtain current-clamp recordings. An extracellular glass stimulating electrode filled with artificial cerebrospinal fluid was placed at the same layer of the pyramidal cell 100–200 μm away from the recording site. Presynaptic axons were stimulated by using current-pulse stimuli [duration = 150 μs, amplitude = 5–20 μA, frequency = 0.1 Hz for measurement of excitatory postsynaptic potentials (EPSPs) before and after conditioning] delivered by a constant-current stimulator. Because STDP typically requires cooperative inputs (10), we adjusted the stimulation intensity to elicit EPSPs with amplitudes >1.5 mV. A glass pipette (tip diameter 20 μm) filled with 5 mM bicuculline was placed near the soma of the pyramidal neuron being recorded to reduce local inhibition without inducing epileptiform activity (5). In a handful of cases, we bath-applied bicuculline (5 μM) instead. To induce STDP, we paired EPSPs with postsynaptic spikes for 50 repetitions (5, 10) at 0.1–1 Hz. Postsynaptic APs were induced by using periodic current-pulses (duration = 5 ms) injected via the recording electrode into the soma. After 50 pairs, test stimuli were delivered to the presynaptic axons at 0.1 Hz in the absence of postsynaptic spikes for at least 30 min. To measure STDP, we compared the maximal rising slope of the evoked EPSP, recorded between the end of the stimulus artifact and the peak of the EPSP, before and after the conditioning pairs. Results were the same when we examined

Conflict of interest statement: No conflicts declared.

Abbreviations: AP, action potential; EC, entorhinal cortex; EPSP, excitatory postsynaptic potential; LTD, long-term depression; LTP, long-term potentiation; STDP, spike-timing-dependent plasticity; TEA, tetraethylammonium; VDCC, voltage-dependent calcium channel.

*To whom correspondence should be addressed at: Department of Biomedical Engineering, Boston University, 44 Cummington Street, Boston, MA 02215. E-mail: jwhite@bu.edu.

© 2005 by The National Academy of Sciences of the USA

changes in EPSP amplitude (data not shown). Spike half-width was defined as a spike's duration at half-spike amplitude, measured from threshold voltage (defined as the voltage at which the spike induced an inflection in the trace) to peak. Reported half-widths are from isolated spikes (i.e., spikes evoked without accompanying EPSPs).

Input resistance, resting membrane potential, and spike half-width were monitored throughout the recording session to ensure stability of recordings. Except in cases in which we purposefully modulated spike width, data were discarded when any of these measures changed by more than 10% during the recording session. Data are reported statistically as mean \pm SEM.

Optical Imaging. Neurons were loaded intracellularly for 1 h with intracellular fluid containing 20 μ M calcium green-1, hexapotassium salt ($K_D = 190$ nM; Molecular Probes). Neurons were imaged by using an Axioskop 2FS+ microscope (Zeiss) equipped with a 150-W arc-lamp from Opti-Quip (Highland Mills, NY) and an epifluorescence illumination cube (exciter = 480/40 nm, dichroic = 505 nm, and emitter = 535/50 nm; Chroma Technology, Rockingham, VT) and imaged with a NeuroCCD-256-SM charge-coupled device camera (Red Shirt Imaging, Fairfield, CT). The region of interest (ROI) was selected around the apical dendrite of the cell. Before the experiment, we verified that the baseline fluorescence within the ROI had stabilized, and the change in fluorescence from each AP fluctuated by $<5\%$ from trial to trial. The protocol for the experiment consisted of taking sets of five trials containing 70 frames recorded at 25–100 Hz while simultaneously recording the electrical activity of the cell at 6.4 kHz. The neuron was stimulated at the onset of the 20th frame with a pulse of current (duration = 10 ms, amplitude = 2–5 nA). The calcium signal was measured by subtracting the average baseline $\Delta F/F$ from the peak $\Delta F/F$ observed in a 50-ms window after the AP. Trials were taken every 3 seconds, and a set of five trials was taken every minute. A baseline of three to five sets was established before 10 mM tetraethylammonium (TEA) was washed in for 3 min and then washed off. In TEA, cells occasionally fired bursts or did not fire; only trials in which a single AP was recorded were included in the results. Results were corrected for photobleaching by detrending using an exponential fit to the baseline and wash-out data. Results were normalized by the baseline response.

Modeling. In the proposed model, described in detail in *Supporting Text*, which is published as supporting information on the PNAS web site, and shown in cartoon form in Fig. 3c, simulated NMDA receptors included glutamate-mediated activation and instantaneous magnesium block (18). Postsynaptic APs were modeled as biexponential waveforms that matched dendritic recordings (19); the decay-time constant was adjusted to match APs of normal and broad half-width. The LTD signal was linearly related to the peak Ca^{2+} waveform from NMDA receptors; the LTP signal was generated by passing the peak Ca^{2+} concentration through a quadratic nonlinearity. The Ca^{2+} signal from voltage-dependent Ca^{2+} channels (VDCCs) suppressed the input signal from NMDA receptors to the LTP pathway. This suppression signal was a biexponential signal with a delay of 0.5 ms, a rising-time constant of 2 ms, and a decay-time constant of 20 ms. Although our implementation was generated under the assumption that changes in dendritic-spike width mirror those measured in the soma, the only critical feature is that dendritic Ca^{2+} transients covary with somatic AP width (Fig. 3a).

Results

STDP Depends on Spike Width in Layer II/III Pyramidal Neurons of the Rat EC. In brain slices of the EC, we recorded from layer II/III pyramidal cells. To test whether the timing of pre- and postsyn-

aptic activation contributes to the direction of synaptic modification in the superficial layer of EC, we paired pre- and postsynaptic APs at a given time difference. When the onset of EPSPs preceded the peak of postsynaptic APs (positive spike timing), we typically observed a persistent enhancement of the slope of EPSPs after pairing (Fig. 1a; EPSP slope in this example before pairing, 0.77 ± 0.024 V/s; after pairing, 1.09 ± 0.023 V/s; $P < 0.001$, Wilcoxon rank-sum test). In contrast, pairing with negative spike timing typically led to long-lasting depression of the slope of EPSPs (Fig. 1b; EPSP slope in this example before pairing, 1.77 ± 0.034 V/s; after pairing, 1.30 ± 0.020 V/s; $P < 0.001$, Wilcoxon rank-sum test). The relationship between synaptic modifications and the relative timing of pre- and postsynaptic activation under these conditions is shown in Fig. 2b (blue symbols). The STDP profile is generally very similar to those seen in other cortical areas (5, 10).

Surprisingly, there is a correlation between the direction of synaptic modification and the half-width of the postsynaptic AP measured at the soma (Fig. 1). For cases in which the half-width of the AP exceeded 1.5 ms (1.75 ± 0.12 ms, $n = 4$), pairing with positive timing led to LTD instead of LTP in 4 of 4 cases (e.g., Fig. 1c; EPSP slope in this example before pairing, 1.09 ± 0.026 V/s; after pairing, 0.86 ± 0.011 V/s; $P < 0.001$, Wilcoxon rank-sum test). For cases with AP half-width <1.5 ms (1.18 ± 0.044 ms, $n = 19$), positive timing induced clear LTD in only 3 of 19 cases. Pairing in the negative timing window gave rise to LTD for cells with both broad APs (3 of 3 cases, e.g., Fig. 1d; EPSP slope in this example before pairing, 2.13 ± 0.12 V/s; after pairing, 1.79 ± 0.028 V/s; $P < 0.001$, Wilcoxon rank-sum test) or regular APs (5 of 6 cases). Broad and regular-width spikes did not differ in amplitude (for regular-width spikes, 68.7 ± 2.3 mV, $n = 19$; for broad spikes, 69.5 ± 2.6 mV, $n = 4$).

To examine the relationship between spike width and STDP in a larger number of cases, we broadened APs by using intracellular TEA (10 mM), which blocks K^+ channels intracellularly or extracellularly with similar affinity (20). On average, intracellular TEA broadened AP half-width by 50% (Fig. 2a). Over the population of recordings in control conditions and in TEA, LTP can be induced only when the half-width of APs is <1.5 ms (filled red and blue symbols, Fig. 2b). For cases with AP half-width >1.5 ms (open red and blue symbols, Fig. 2b), the STDP curve is more dominated by LTD for both negative and positive timing. The difference in STDP outcomes based on spike width is statistically highly significant ($P < 0.01$, Wilcoxon rank-sum test; Fig. 2c).

AP-Induced Ca^{2+} Transients Modulate STDP. The fact that broader somatic spikes lead to enhanced LTD is counter to what one would predict from the Ca^{2+} peak-detector model. Manipulations that broaden somatic spikes are likely to broaden dendritic spikes as well (21). Broadened dendritic spikes should induce larger dendritic Ca^{2+} transients (21), because the broader spike exposes both NMDA receptors and VDCCs to depolarized potentials for a longer period. These enhanced Ca^{2+} transients should, in turn, enhance LTP, in accordance with the calcium-peak-detector model commonly used to model both conventional and timing-dependent synaptic plasticity (3, 12–14, 22).

We directly examined the effects of somatic spike width on the amplitude of the dendritic Ca^{2+} transient in imaging experiments. In these experiments, we washed in TEA (10 mM) and examined the relationship between somatic spike half-width and the peak of the dendritic Ca^{2+} transient in single cells. In many cases, we blocked ionotropic synaptic transmission to ensure that the observed effects of TEA on spike width and dendritic Ca^{2+} transients were not induced by network effects. In 6 of 6 cases (e.g., Fig. 3a), the Ca^{2+} transient was significantly larger ($P < 0.01$, Wilcoxon rank-sum test) in the presence of TEA than in control conditions. The relationship between AP half-width and

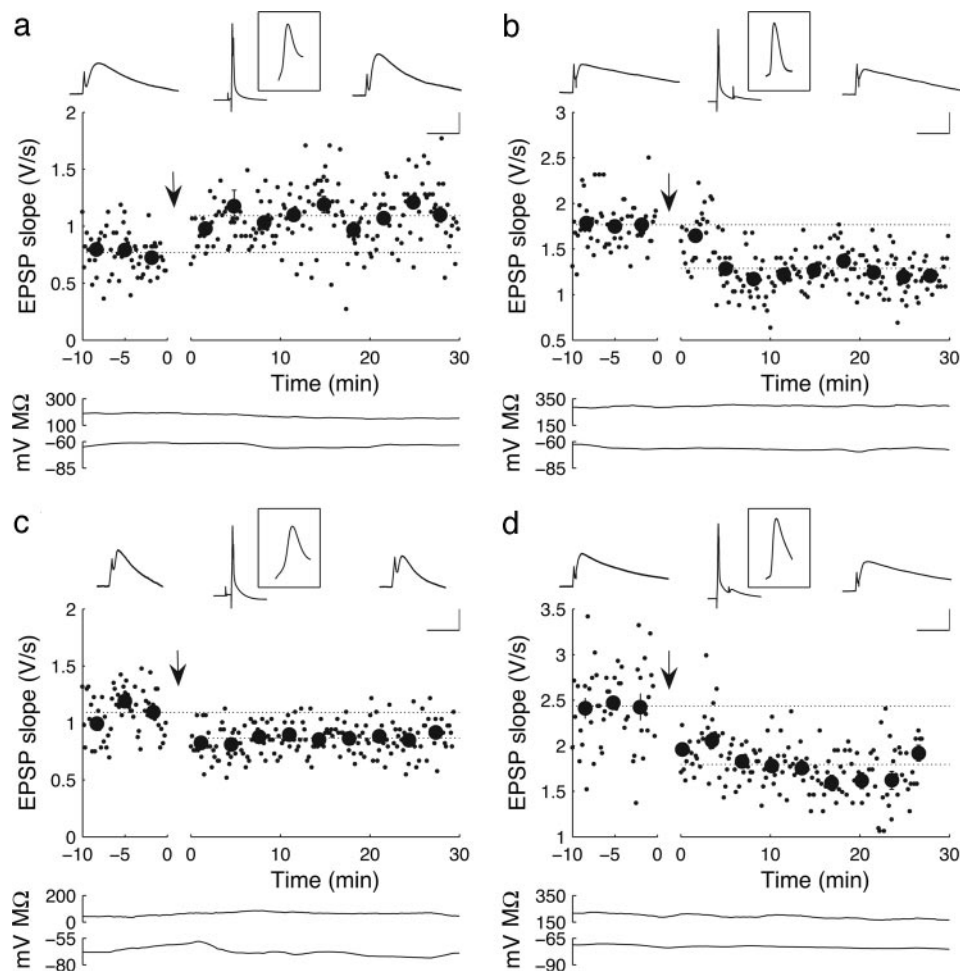


Fig. 1. STDP depends on spike width in layer II/III pyramidal neurons of the rat EC. (a) LTP is induced when EPSPs and postsynaptic APs are paired with positive timing (+10 ms) in a cell with AP half-width of 1.3 ms. Small data points show the maximum rising slope of EPSPs elicited by test stimuli (0.1 Hz); large data points are the mean \pm SD of groups of 20 measurements. Traces above represent average ($n = 20$) EPSPs recorded 5 min before pairing, average AP-EPSP pairs recorded during pairing, and average EPSPs recorded 20 min after pairing. (Inset Top) The average spike paired with the EPSPs. (Bottom) Traces show the input resistance and resting potential. [Scale bar = 1.2 mV, 30 ms (EPSPs); 22 mV, 75 ms (pairing); 22 mV, 3.7 ms (Inset).] (b) LTD is induced with negative timing (-30 ms) in a cell with spike half-width of 1.2 ms. (Scale bar as in a, except that the scale bar for EPSPs is 3 mV.) (c) LTD is induced in a cell with broad spikes (1.7 ms), even though APs and synaptic inputs were paired with positive timing (+20 ms). (Scale bar as in a.) (d) LTD is induced by pairing with negative timing (-20 ms) in a cell with spike half-width of 1.6 ms. (Scale bar as in a, except that the scale bar for EPSPs is 4 mV.)

the peak of the Ca^{2+} transient is approximately linear (average $R = 0.77$; $n = 6$). These results demonstrate that manipulations of AP width lead to expected increases in the amplitudes of Ca^{2+} transients, implying that timing-dependent LTP and LTD do not operate by simply thresholding the dendritic Ca^{2+} transient.

We explored the role of Ca^{2+} in STDP in more detail. Intracellular administration of the Ca^{2+} chelator 1,2-bis(2-aminophenoxy)ethane- N,N,N',N' -tetraacetate (10 mM) reduces the amount of STDP-induced LTP for $\Delta t = 15$ ms from 17.5 ± 17.5 ($n = 4$) to -5.69 ± 4.5 ($n = 5$). This reduction in LTP is significant ($P < 0.05$) when analyzed by using the one-tailed Wilcoxon rank-sum test. The two most likely sources of dendritic Ca^{2+} influx are NMDA receptors and VDCCs. Two-amino-5-phosphonovalerate (30 μM), which blocks Ca^{2+} influx through NMDA receptors, prevented the induction of STDP in all conditions (Fig. 3b), indicating that STDP in EC is NMDA-receptor-dependent. Nifedipine (10 μM), an L-type (Ca_v1) Ca^{2+} channel blocker, generally tilts the balance of STDP toward potentiation (compare results in nifedipine with those in control in Fig. 3b), implying that Ca^{2+} flux through postsynaptic VDCCs provides feedback that inhibits LTP and/or enhances LTD. In 3 of 3 cases, the spike-evoked Ca^{2+} transient was significantly

inhibited ($P < 0.01$, Wilcoxon rank-sum test) by nifedipine (Fig. 3b Inset). Blocking Ca_v1 Ca^{2+} channels did not affect synaptic transmission and AP generation: both AP duration ($99.5 \pm 3.2\%$ of the control, $n = 4$; $P \approx 1$, paired Wilcoxon rank-sum test) and EPSP slope ($98.04 \pm 10.6\%$ of the control, $n = 4$; $P \approx 1$, paired Wilcoxon rank-sum test) remained constant after wash-in of nifedipine. The effects of nifedipine on STDP are statistically significant in most cases ($P < 0.05$, Wilcoxon rank-sum test). In particular, entorhinal pyramidal cells show exclusive LTP for positive timing in nifedipine. For negative timing, blocking Ca_v1 channels reduces or eliminates LTD in our preparation (Fig. 3b) as well as visual cortex (23) and hippocampal culture (2).

Based on our results from manipulations of spike width and dendritic Ca^{2+} channels, we modified the Ca^{2+} -peak-detector model to include feedback from VDCCs that favors LTD over LTP. The proposed model is shown in Fig. 3c. We build peak detection into the model by making LTP and LTD depend quadratically and linearly, respectively, on the Ca^{2+} waveform through NMDA receptors. Thus, in the absence of feedback from VDCCs, small transients generate a larger LTD signal, whereas large transients generate a larger LTP signal. This nonlinear gain for LTP is qualitatively compatible with the

LTD when the spike timing is negative and a conversion of LTD to LTP when EPSPs precedes the broadened APs (Fig. 3*b*, red boxes). For three of four conditions, the quantitative match between the model and the data in Fig. 3*b* is excellent. In the fourth case (regular spikes, negative timing), the model predicts the trend correctly but overestimates the size of the effect of blocking VDCCs. Interestingly, blocking VDCCs eliminates left-hand-side LTD in other experimental studies (2, 23).

Discussion

By investigating STDP on pyramidal neurons with constitutively or pharmacologically broadened APs, we showed that the postsynaptic AP width is critical for the direction of synaptic modification in the EC. Broad postsynaptic APs shift the balance of STDP toward depression. When the half-width of an AP exceeds 1.5 ms, no timing-dependent LTP is observed. Ca^{2+} imaging experiments on the proximal dendrites showed that dendritic Ca^{2+} transients are proportional to the half-width of APs recorded from the soma. Our results imply that enhanced VDCC-mediated Ca^{2+} transients are correlated with diminished LTP and enhanced LTD. This result contradicts the Ca^{2+} threshold-detector model, the most prevalent model linking Ca^{2+} signals to LTP. Other results call the peak-detector model into question as well. First, the peak-detector model predicts LTD when presynaptic APs precede postsynaptic APs by a sufficiently long time interval; such results are not seen in most experimental data, including ours. (See ref. 8 for a potential resolution of this discrepancy.) Second, triplets of pre-post-presynaptic (or post-pre-postsynaptic) APs, which are likely to lead to larger Ca^{2+} transients in the dendrite than do doublets of APs, often induce LTD (10, 25, 26).

The essential feature of our algorithm for STDP is that VDCC-mediated Ca^{2+} fluxes, evoked by postsynaptic APs, shift the balance in metabolic signals leading to LTP and LTD toward LTD. The duration of this effect determines the temporal extent of the LTD window for negative timing. Such an algorithm could arise from a number of mechanisms, including (as pictured in Fig. 3*c*) divergent signaling pathways, driven by a single NMDA-mediated Ca^{2+} flux but differentially modulated by VDCC-driven transients. Another possibility involves multiple pools or classes of NMDA receptors, tied to different outcomes in terms of plasticity (27, 28) and differentially modulated by feedback from VDCCs. A model of this form would require modification of the diagram in Fig. 3*c* to include these two pools, perhaps in

different cellular locations (28) but would not necessarily require any changes in the computational model.

Although we are not in a position to construct a detailed, mechanistic model of STDP induction, we can rule out some simple alternatives to the model of Fig. 3*c*. Models that did not include VDCC-mediated suppression of the LTP pathway were unable to account for the enhancement of LTD in response to spike broadening. Models in which VDCC-mediated currents generally suppressed NMDA receptors (29–31) and reduced both LTP and LTD were also ineffective in fitting our data. Although these models could partially account for enhanced LTD, with spike broadening for positive timing, they could not simultaneously account for the depression-enhancing effects of spike broadening for negative timing (data in Fig. 3*b*; simulation results not shown). Our data are also incompatible with the specific multidetector recently proposed by Bi and colleagues (25, 26), in which a low- Ca^{2+} -threshold mechanism leads to a “veto” of LTD. Like the standard Ca^{2+} peak-detector model, we believe that the Bi model is incapable of accounting for increasing LTD with increased spike width, because spike broadening and subsequent enhancement of the Ca^{2+} transient would only increase the degree of veto of LTD. However, our data are supportive of the general hypothesis from Bi and Buonomano (25, 26, 32) that multiple, spatially segregated Ca^{2+} signals are necessary to account for the properties of STDP. In particular, we require that the modulatory VDCC-mediated Ca^{2+} transient be segregated from NMDA-mediated signal. Imaging data support such segregation: In neocortical pyramidal cells, Ca^{2+} transients evoked by postsynaptic APs give rise to Ca^{2+} transients in the dendritic trunk and spines, whereas EPSP-evoked transients are confined to the spine head (15).

Our findings suggest that modulation of spike width (e.g., through phosphorylation- or history-dependent mechanisms) could provide a way to alter the properties of long-term synaptic plasticity. Feedback from VDCC-mediated Ca^{2+} transients is likely to be an important factor in other circumstances as well. For example, induction of LTP in CA1 pyramidal cells leads to local enhancement of the dendritic Ca^{2+} transient evoked by back-propagating APs near the potentiated synapse (33). Under these circumstances, feedback from VDCCs may tilt the balance of potentiated synapses back toward synaptic depression.

We thank B. G. Burton, M. E. Hasselmo, D. Johnston, and K. Lillis for helpful discussions and comments. This work was supported by National Institutes of Health Grant NS34425.

- Bi, G. & Poo, M. (2001) *Annu. Rev. Neurosci.* **24**, 139–166.
- Bi, G. Q. & Poo, M. M. (1998) *J. Neurosci.* **18**, 10464–10472.
- Dan, Y. & Poo, M. M. (2004) *Neuron* **44**, 23–30.
- Debanne, D., Gahwiler, B. H. & Thompson, S. M. (1998) *J. Physiol. (London)* **507**, 237–247.
- Feldman, D. E. (2000) *Neuron* **27**, 45–56.
- Magee, J. C. & Johnston, D. (1997) *Science* **275**, 209–213.
- Markram, H., Lubke, J., Frotscher, M. & Sakmann, B. (1997) *Science* **275**, 213–215.
- Nishiyama, M., Hong, K., Mikoshiba, K., Poo, M. M. & Kato, K. (2000) *Nature* **408**, 584–588.
- Sjöström, P. J. & Nelson, S. B. (2002) *Curr. Opin. Neurobiol.* **12**, 305–314.
- Sjöström, P. J., Turrigiano, G. G. & Nelson, S. B. (2001) *Neuron* **32**, 1149–1164.
- Zhang, L. I., Tao, H. W., Holt, C. E., Harris, W. A. & Poo, M. (1998) *Nature* **395**, 37–44.
- Abarbanel, H. D., Huerta, R. & Rabinovich, M. I. (2002) *Proc. Natl. Acad. Sci. USA* **99**, 10132–10137.
- Artola, A. & Singer, W. (1993) *Trends Neurosci.* **16**, 480–487.
- Shouval, H. Z., Bear, M. F. & Cooper, L. N. (2002) *Proc. Natl. Acad. Sci. USA* **99**, 10831–10836.
- Koester, H. J. & Sakmann, B. (1998) *Proc. Natl. Acad. Sci. USA* **95**, 9596–9601.
- Yun, S. H., Mook-Jung, I. & Jung, M. W. (2002) *J. Neurosci.* **22**, RC214.
- Netoff, T. I., Banks, M. I., Dorval, A. D., Acker, C. D., Haas, J. S., Kopell, N. & White, J. A. (2005) *J. Neurophysiol.* **93**, 1197–1208.
- Destexhe, A., Mainen, Z. F. & Sejnowski, T. J. (1998) in *Methods in Neuronal Modeling: from Ions to Networks*, eds Koch, C. & Segev, I. (MIT Press, Cambridge, MA), pp. 1–26.
- Hoffman, D. A., Magee, J. C., Colbert, C. M. & Johnston, D. (1997) *Nature* **387**, 869–875.
- Hille, B. (2001) *Ion Channels of Excitable Membranes* (Sinauer, Sunderland, MA), 3rd Ed., pp. 555–556.
- Korngreen, A., Kaiser, K. M. & Zilberter, Y. (2005) *J. Physiol. (London)* **562**, 421–437.
- Lisman, J. (1989) *Proc. Natl. Acad. Sci. USA* **86**, 9574–9578.
- Froemke, R. C., Poo, M. M. & Dan, Y. (2005) *Nature* **434**, 221–225.
- Malenka, R. C. & Nicoll, R. A. (1999) *Science* **285**, 1870–1874.
- Rubin, J. E., Gerkin, R. C., Bi, G. Q. & Chow, C. C. (2005) *J. Neurophysiol.* **93**, 2600–2613.
- Bi, G. Q. & Rubin, J. (2005) *Trends Neurosci.* **28**, 222–228.
- Liu, L., Wong, T. P., Pozza, M. F., Lingenhoeh, K., Wang, Y., Sheng, M., Auberson, Y. P. & Wang, Y. T. (2004) *Science* **304**, 1021–1024.
- Sjöström, P. J., Turrigiano, G. G. & Nelson, S. B. (2003) *Neuron* **39**, 641–654.
- Legendre, P., Rosenmund, C. & Westbrook, G. L. (1993) *J. Neurosci.* **13**, 674–684.
- Tong, G., Shepherd, D. & Jahr, C. E. (1995) *Science* **267**, 1510–1512.
- Zucker, R. S. (1999) *Curr. Opin. Neurobiol.* **9**, 305–313.
- Karmarkar, U. R. & Buonomano, D. V. (2002) *J. Neurophysiol.* **88**, 507–513.
- Frick, A., Magee, J. & Johnston, D. (2004) *Nat. Neurosci.* **7**, 126–135.